

Dynamical Lamb effect versus dissipation in superconducting quantum circuitsA. A. Zhukov,^{1,2} D. S. Shapiro,^{1,3,4,5} W. V. Pogosov,^{1,4,6} and Yu. E. Lozovik^{1,7,8}¹*N. L. Dukhov All-Russia Research Institute of Automatics, 127055 Moscow, Russia*²*National Research Nuclear University (MEPhI), 115409 Moscow, Russia*³*V. A. Kotel'nikov Institute of Radio Engineering and Electronics, Russian Academy of Sciences, 125009 Moscow, Russia*⁴*Moscow Institute of Physics and Technology, Dolgoprudny, 141700 Moscow Region, Russia*⁵*National University of Science and Technology MISIS, 119049 Moscow, Russia*⁶*Institute for Theoretical and Applied Electrodynamics, Russian Academy of Sciences, 125412 Moscow, Russia*⁷*Institute of Spectroscopy, Russian Academy of Sciences, 142190 Moscow Region, Troitsk, Russia*⁸*Moscow Institute of Electronics and Mathematics, National Research University Higher School of Economics, 101000 Moscow, Russia*

(Received 7 March 2016; published 27 June 2016)

Superconducting circuits provide a new platform for study of nonstationary cavity QED phenomena. An example of such a phenomenon is the dynamical Lamb effect, which is the parametric excitation of an atom due to nonadiabatic modulation of its Lamb shift. This effect was initially introduced for a natural atom in a varying cavity, while we suggest its realization in a superconducting qubit-cavity system with dynamically tunable coupling. In the present paper, we study the interplay between the dynamical Lamb effect and the energy dissipation, which is unavoidable in realistic systems. We find that despite naive expectations, this interplay can lead to unexpected dynamical regimes. One of the most striking results is that photon generation from vacuum can be strongly enhanced due to qubit relaxation, which opens another channel for such a process. We also show that dissipation in the cavity can increase the qubit excited-state population. Our results can be used for experimental observation and investigation of the dynamical Lamb effect and accompanying quantum effects.

DOI: [10.1103/PhysRevA.93.063845](https://doi.org/10.1103/PhysRevA.93.063845)**I. INTRODUCTION**

Superconducting circuits can be exploited for experimental investigation of cavity quantum electrodynamical (QED) effects [1]. This possibility is due to the recent progress in fabrication methods and quantum field control, which allows one to use superconducting systems in quantum information and computation [2–7]. The transfer of information can be efficiently implemented provided dissipation effects and external noise are ruled out, while this problem is known to be quite difficult to solve [8]. Obviously, similar requirements have to be fulfilled for QED effects to be observed in experiments.

Several years ago the first observation of one of the most intriguing nonstationary QED phenomena, known as the dynamical Casimir effect, was reported [9,10]. It is quite remarkable that it was observed for the first time in superconducting systems although it has been predicted for systems seemingly very distinct from such circuits [11]. Being nonstationary, the dynamical Casimir effect differs from the static Casimir effect. The static Casimir effect is manifested as an attraction of two static mirrors due to the zero-point fluctuations of the photon field confined between them. These vacuum fluctuations contribute also to another well-known static QED effect: Lamb shift of the atom spectrum. This shift exists not only for natural atoms, but also for artificial superconducting “atoms” (qubits) coupled to resonators [12]. Moreover, in contrast to natural atoms, the effect can be significantly enhanced, since a regime of strong qubit-cavity coupling is achievable in such systems.

The dynamical Casimir effect was initially predicted to occur provided the mirrors are moving with respect to each other. This motion leads to a modulation of the allowed photon wave vectors, as dictated by the quantization conditions. As a

result, real photons are generated from a vacuum between the mirrors, thus parametrically amplifying vacuum fluctuations. In order to produce a feasible photon emission rate, one has to move mirrors at velocities approaching the speed of light. For massive mirrors, this requirement is challenging for the current experimental facilities. That is why various indirect schemes have been suggested [13–16], among which we mention the modulation of electromagnetic properties of the cavity walls and the use of acoustic waves and nanomechanical resonators. One such proposal was to modulate the inductance of a superconducting quantum interference device (SQUID) connected to a coplanar waveguide [17]. Such a modulation can be treated as a change in the electrical length of the waveguide which is accompanied by the desired variation of boundary conditions. Since no motion of massive objects is involved, a very fast modulation rate can be achieved.

We wish to stress that the dynamical Casimir effect is just one example of a large class of nonstationary QED effects in which vacuum amplification is expected to play a major role [1]. The best-known effects of this kind are the Unruh effect [18] and Hawking radiation [19]. None of these phenomena has been observed so far except for the dynamical Casimir effect.

Very rich behavior is also demonstrated by nonstationary cavities containing a single atom or an ensemble of such atoms, thanks to matter-light coupling (see, e.g., Refs. [20–27]). The simplest possible system of this kind is a single-mode cavity with a time-dependent frequency, which contains a two-level system. A cavity with a nonadiabatically modulated frequency is similar to a parametrically driven harmonic oscillator. Such a modulation leads to the generation of Casimir photons, which are naturally absorbed by the atom, resulting in its excitation [22]. A precise analysis [23], however, shows that

there is another channel of atom excitation which is due to nonadiabatic modulation of its Lamb shift. This effect is related to the static Lamb shift in a similar way as the dynamical Casimir effect is related to the static Casimir effect. For this reason, it was suggested in Ref. [23] that this phenomenon be termed the *dynamical Lamb effect*.

Unfortunately, experimentally it seems to be quite difficult to isolate the channel of atom excitation due to the absorption of Casimir photons from the mechanism due to the dynamical Lamb effect, since these two excitation channels always appear together in experiments with nonstationary cavities, in which their frequencies experience external variations. Fortunately, instead of real atoms it is possible to use artificial “atoms” made of superconducting circuits with Josephson junctions. This opportunity is very attractive because of the high flexibility of such circuits. Two-level superconducting artificial atoms are used nowadays as qubits for purposes of quantum computation. Being macroscopic in size, they can demonstrate quantum behavior on rather long time scales, approaching hundreds of microseconds for state-of-the-art devices. Quality factors of the available microwave resonators are of the order of 10^6 , so that a coupled qubit-cavity system can behave quantum mechanically during the time intervals needed to perform hundreds or thousands of quantum gates [5].

Moreover, it is known that coupled systems of superconducting resonators and qubits can be fabricated as *dynamically* tunable *in situ* during experiments. It was demonstrated that not only can the resonator frequency and the qubit excitation energy be modulated, but also one can change the vacuum Rabi frequency determined by the strength of the qubit-resonator coupling. This modulation can be achieved using either flux qubits with an additional SQUID or two strongly coupled charge qubits (transmons), from which a single effective two-level system can be created (see, e.g., Refs. [28–30]). Thus it is possible not only to change several parameters simultaneously by perturbing the whole system, but also to modulate a particular *single* parameter.

This remarkable opportunity opens the possibility of full isolation of the mechanism of qubit excitation due to the dynamical Lamb effect from the channel of its excitation due to the absorption of Casimir photons, as suggested recently in Ref. [31]. Indeed, if one modulates only the qubit-resonator coupling and does not change the resonator frequency, no Casimir photons appear. Nevertheless, the qubit can be parametrically excited since it somehow “feels” a nonadiabatic change of its Lamb shift. In order to enhance the effect and to increase the qubit excited-state population, it was suggested in [31] to modulate the resonator-qubit coupling periodically with twice the resonator frequency, while the qubit and resonator are in full resonance. However, in [31] dissipation in the qubit-resonator coupled system was completely ignored.

The major aim of the present paper is to treat the interplay between the dynamical Lamb effect and the dissipation within the realization proposed in Ref. [31]. The naive expectation is that dissipation must always suppress this purely quantum effect, as well as the process of photon generation from a vacuum. In particular, relaxation of qubits is opposite to the qubit excitation process, induced by the dynamical Lamb effect, since it leads to qubit de-excitation. In reality, we

find that the effect of dissipation is far more complex and it results in several highly unexpected dynamical regimes including enhanced generation of photons from a vacuum. Another regime resembles a parametric down conversion since it results in the generation of photon pairs at frequencies lower than the pump frequency.

This paper is organized as follows. In Sec. II, we describe the system under consideration and outline our theoretical model. In Sec. III, we present a simple toy model which allows us to understand some important features of the dynamical behavior of our system without performing numerical simulations and under the assumption that the decay rate in the cavity can be neglected. The results of such simulations under the same assumption are then presented in Sec. IV. Section V deals with the analysis of the effect of cavity relaxation. In Sec. VI we apply an alternative method to solve a problem applicable for the stationary limit after stabilization in order to cross-check our main results. We conclude in Sec. VII.

II. HAMILTONIAN AND BASIC EQUATIONS

We focus on superconducting circuits which consist of flux or charge qubits (transmons). This two-level system is coupled dynamically to a high-quality coplanar waveguide, playing the role of a single-mode cavity in optical systems. Qubit and waveguide are spatially separated on a chip; indeed, coupling between them can be organized by auxiliary SQUID or by means of other methods [28,30]. Current superconducting technologies allow the realization of architectures where qubit-cavity coupling can be switched on and off or tuned at gigahertz frequencies, while the amplitude can be varied at values up to 100 MHz. As can be expected, near-future technologies will be able to impose even more adjustable modulations.

We describe the photon mode and qubit (at frequencies ω and ϵ , respectively, which are of the order of several gigahertz) by means of the Rabi model [32,33], known from quantum optics, taking into account the dynamically tunable coupling energy $g(t)$. The total Hamiltonian of this system reads

$$H(t) = \omega a^\dagger a + \frac{1}{2}\epsilon(1 + \sigma_3) + V(t), \quad (1)$$

where a^\dagger and a are secondary quantized photon creation and annihilation operators and $\sigma_3 = 2\sigma_+\sigma_- - 1, \sigma_+, \sigma_-$ are Pauli operators related to the qubit degrees of freedom. The nonstationary operator $V(t)$ describes the dynamical qubit-cavity coupling

$$V(t) = g(t)(a + a^\dagger)(\sigma_- + \sigma_+), \quad (2)$$

where $(a + a^\dagger)$ and $(\sigma_- + \sigma_+)$ are related to the electric-field and dipole moment operators, respectively.

This qubit-cavity interaction operator can be divided into two parts,

$$V(t) = V_1(t) + V_2(t), \quad (3)$$

where

$$V_1(t) = g(t)(a\sigma_+ + a^\dagger\sigma_-) \quad (4)$$

is responsible for the well-known rotating-wave approximation, provided V_2 is dropped, while V_2 is given by

$$V_2(t) = g(t)(a^\dagger \sigma_+ + a \sigma_-). \quad (5)$$

This counter-rotating-wave term is usually neglected.

The term V_1 in the Hamiltonian conserves the total number of excitations in the system, and in the stationary case $V_1(t) = \text{const}$ it provides the exactly solvable Jaynes-Cummings model, which is well justified near resonance, $\omega \simeq \epsilon$, and for weakly interacting systems, $g \ll \omega$. The counter-rotating-wave term V_2 violates the conservation of the excitation number, while it conserves the parity. This term plays a central role in our treatments because it leads to the dynamical Lamb effect. Namely, nonadiabatic modulation of $V_2(t)$ provides qubit excitation with simultaneous photon creation [23,31].

In our previous paper [31], we took into account instantaneous and periodic switching of the $g(t)$ of particular rectangular shapes, which provides its nonadiabatic modulation, because the dynamical Lamb effect occurs upon nonadiabatic changes in a system's parameters [23]. We considered both single switching, as $g(t) = g\theta(t)$, and periodic switching, as $g(t) = g\theta(\cos 2\omega t)$, where the last modulation resulted in a parametric pumping of the system, leading to a dramatic increase in the effect in the case of full resonance $\omega = \epsilon$. This behavior has some similarities with the so-called anti-Jaynes-Cummings regime described in Ref. [26], in which a single photon and one atomic excitation are created. In the present work, we focus on the same most efficient

2ω -periodic modulations, whereas a particular shape of $g(t)$ can be arbitrary. In our solution, a major role is played by two Fourier components of the $g(t)$, $q = g_0$ and $p = g_{2\omega}$, which control the dynamics in the regime of weak qubit-cavity coupling. For the above modulation containing periodic switching on and off, these two parameters are $p = 0.5$ and $q = 1/\pi$. A large portion of our results is presented using these particular values of p and q , since such results turn out to be rather typical for the domain of parameters $p > q$. Moreover, this choice allows us to keep a direct link with Refs. [23] and [31]. We also assume that relaxation in the qubit exceeds losses in the photon mode, i.e., $\gamma \gg \kappa$, which might be related to the experimental situation with $\gamma \sim 1$ MHz for transmons and $\kappa \sim 10$ kHz for the cavity.

The dynamics of our system in the presence of energy dissipation can be found from the Lindblad equation, which reads

$$\partial_t \rho(t) - \Gamma(\rho(t)) = -i[H(t), \rho(t)], \quad (6)$$

where relaxation is described by means of the matrix

$$\Gamma(\rho) = \kappa(2a\rho a^\dagger - a^\dagger a\rho - \rho a^\dagger a) + \gamma(2\sigma_- \rho \sigma_+ - \sigma_+ \sigma_- \rho - \rho \sigma_+ \sigma_-). \quad (7)$$

In superconducting systems, dissipation of the qubit degrees of freedom is typically much stronger than cavity relaxation. We focus mostly on this situation, while the effect of cavity relaxation is analyzed in Sec. V.

In explicit form, master equations for the density matrix operator $\rho(t)$ neglecting cavity relaxation κ read as

$$\begin{aligned} i\dot{\rho}_{m,n}^{gg} &= \rho_{m,n}^{gg} \omega(n-m) + i\gamma\rho_{m,n}^{ee} + g(t)(\sqrt{n}\rho_{m,n-1}^{ge} + \sqrt{n+1}\rho_{m,n+1}^{ge} - \sqrt{m}\rho_{m-1,n}^{eg} - \sqrt{m+1}\rho_{m+1,n}^{eg}), \\ i\dot{\rho}_{m,n}^{ee} &= \rho_{m,n}^{ee} [\omega(n-m) - i\gamma] + g(t)(\sqrt{n}\rho_{m,n-1}^{eg} + \sqrt{n+1}\rho_{m,n+1}^{eg} - \sqrt{m}\rho_{m-1,n}^{ge} - \sqrt{m+1}\rho_{m+1,n}^{ge}), \\ i\dot{\rho}_{m,n}^{eg} &= \rho_{m,n}^{eg} [\omega(n-m) - \epsilon - i\gamma/2] + g(t)(\sqrt{n}\rho_{m,n-1}^{ee} + \sqrt{n+1}\rho_{m,n+1}^{ee} - \sqrt{m}\rho_{m-1,n}^{gg} - \sqrt{m+1}\rho_{m+1,n}^{gg}), \\ i\dot{\rho}_{m,n}^{ge} &= \rho_{m,n}^{ge} [\omega(n-m) + \epsilon - i\gamma/2] + g(t)(\sqrt{n}\rho_{m,n-1}^{gg} + \sqrt{n+1}\rho_{m,n+1}^{gg} - \sqrt{m}\rho_{m-1,n}^{ee} - \sqrt{m+1}\rho_{m+1,n}^{ee}), \end{aligned} \quad (8)$$

where the superscript indices of density matrix components stand for the qubit ground (g) and excited (e) states, while the subscript indices correspond to the photon numbers. These equations can be solved numerically by truncating the basis for photon states and taking into account some reasonable number of these states. The accuracy can be verified by increasing the number of states in the basis and comparing the results with the results for a smaller basis.

However, before treating these equations, we consider a general structure of bare energy levels and processes in which they participate. These processes are due to the interaction terms V_1 and V_2 in the Hamiltonian, as well as to the decay of the qubit excited state. Figure 1 illustrates the dynamics of the system upon the action of the external driving in the resonant case $\omega = \epsilon$.

In general, it may be expected that there should be a competition between various processes in our system. Namely, there is a purely coherent process of parametric qubit excitation tending to populate states $|n, e\rangle$, n being odd, via the term V_2 in the Hamiltonian, which does not conserve the excitation

number (solid lines), and the excitation-number-conserving term V_1 (dashed lines). This process is considered in our previous paper [31]. Qubit excitation due to the dynamical Lamb effect occurs during this process, thanks to V_2 . There is also a process of decay of the qubit excited state (wavy dotted curves in Fig. 1), which may tend to return the system to the initial state via V_1 . The latter process tries to suppress the dynamical Lamb effect. However, instead of returning to the initial state, the system can again be excited via V_2 , leading to nonzero populations of states $|n, e\rangle$, n being even. A toy model is proposed in the next section in order to describe some aspects of this behavior on the simplest grounds.

III. TOY MODEL

Let us take into account only four bare levels, which have the lowest energy: $|0, g\rangle$, $|0, e\rangle$, $|1, g\rangle$, and $|1, e\rangle$. We choose these levels because the system of these four states already supports two of the most important processes mentioned above: (i) excitation of the system via V_2 , $|0, g\rangle \rightarrow |1, e\rangle$

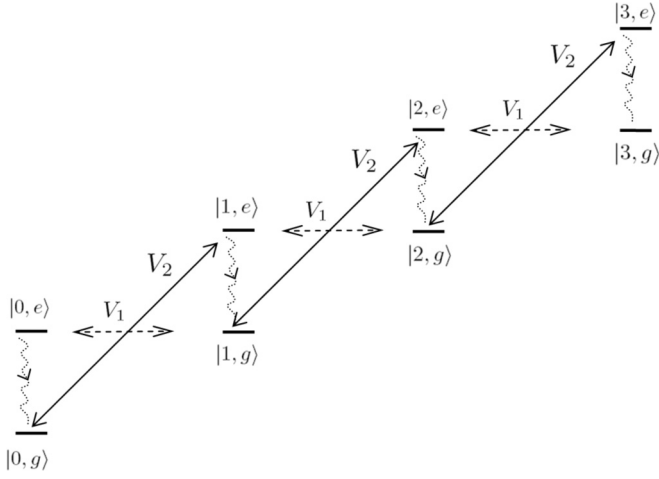


FIG. 1. Structure of the bare energy spectrum in the case of a full cavity-qubit resonance and the main processes induced between bare states due to interaction terms in the Hamiltonian, as well as due to the decay of the qubit excited state (see text).

and (ii) subsequent decay, $|1,e\rangle \rightarrow |0,e\rangle$, accompanied by oscillations between $|0,e\rangle$ and $|1,g\rangle$ due to V_1 . It does not take into account, however, the possibility of a qubit's being excited again by V_2 after the decay of its excited state, since a larger basis is needed to treat it. This process leads to important modifications, as demonstrated in the next section.

The system of these four levels is described by a set of 10 equations for the density matrix components. Actually, in the context of the dynamical Lamb effect, the most important components of the density matrix are those which are responsible for the populations of the above levels. It can be seen from the full set of equations that this set splits into two uncoupled subsets. The subset relevant for the occupation probabilities of two-qubit states are

$$i\dot{\rho}_{0,0}^{gg} = i\gamma\rho_{0,0}^{ee} + g(t)(\rho_{0,1}^{ge} - \rho_{0,1}^{eg*}), \quad (9)$$

$$i\dot{\rho}_{0,0}^{ee} = -i\gamma\rho_{0,0}^{ee} + g(t)(\rho_{0,1}^{eg} - \rho_{0,1}^{eg*}), \quad (10)$$

$$i\dot{\rho}_{1,1}^{gg} = i\gamma\rho_{1,1}^{ee} + g(t)(\rho_{1,0}^{ge} - \rho_{1,0}^{eg*}), \quad (11)$$

$$i\dot{\rho}_{1,1}^{ee} = -i\gamma\rho_{1,1}^{ee} + g(t)(\rho_{1,0}^{eg} - \rho_{1,0}^{eg*}), \quad (12)$$

$$i\dot{\rho}_{0,1}^{eg} = \rho_{0,1}^{eg}(\omega - \varepsilon - i\gamma/2) + g(t)(\rho_{0,0}^{ee} - \rho_{1,1}^{gg}), \quad (13)$$

$$i\dot{\rho}_{0,1}^{ge} = \rho_{0,1}^{ge}(\omega + \varepsilon - i\gamma/2) + g(t)(\rho_{0,0}^{gg} - \rho_{1,1}^{ee}). \quad (14)$$

We hereafter consider the qubit and cavity to be in full resonance, $\omega = \varepsilon$. Let us represent $\rho_{0,1}^{ge}$ by the product of fast- and slow-oscillating factors as

$$\rho_{0,1}^{ge} = \tilde{\rho}_{0,1}^{ge} \exp(-2i\omega t), \quad (15)$$

as suggested by Eq. (14). All other components of the density matrix are free of fast oscillations as seen from Eqs. (9)–(13).

Next, we insert Eq. (15) into Eqs. (9)–(14) and perform an approximate averaging over time. For the time-averaged quantities appearing on the right-hand sides of the resulting

equations we use the uncouplings

$$\begin{aligned} \langle g(t)\tilde{\rho}_{0,1}^{ge} \rangle_t &\simeq \langle g(t) \rangle_t \tilde{\rho}_{0,1}^{ge} \equiv p\tilde{\rho}_{0,1}^{ge}, \\ \langle g(t)\exp(-2i\omega t)\tilde{\rho}_{0,1}^{ge} \rangle_t &\simeq \langle g(t)\exp(-2i\omega t) \rangle_t \tilde{\rho}_{0,1}^{ge} \\ &\equiv q\tilde{\rho}_{0,1}^{ge}, \end{aligned} \quad (16)$$

which are further utilized to separate fast and slow oscillations. It can be proved that they are valid provided $g(t) \ll \omega$. Thus we look for a stationary, in leading order, solution that implies that the left-hand sides of Eqs. (9)–(14) must vanish. Note that we assume the time invariance of $g(t)$: $g(-t) = g(t)$.

We, finally, obtain the following set of linear equations for the stationary solution:

$$i\gamma\rho_{0,0}^{ee} + q(\tilde{\rho}_{0,1}^{ge} - \text{c.c.}) = 0, \quad (17)$$

$$-i\gamma\rho_{0,0}^{ee} + p(\rho_{0,1}^{eg} - \text{c.c.}) = 0, \quad (18)$$

$$-i\gamma\rho_{1,1}^{ee} + p(\rho_{1,0}^{eg} - \text{c.c.}) = 0, \quad (19)$$

$$i\gamma\rho_{1,1}^{ee} + q(\tilde{\rho}_{0,1}^{ge} - \text{c.c.}) = 0, \quad (20)$$

$$-\frac{i\gamma}{2}\rho_{0,1}^{eg} + p(\rho_{0,0}^{ee} - \rho_{1,1}^{gg}) = 0, \quad (21)$$

$$-\frac{i\gamma}{2}\tilde{\rho}_{0,1}^{ge} + q(\rho_{0,0}^{gg} - \rho_{1,1}^{ee}) = 0. \quad (22)$$

By solving this linear system of equations, we readily express populations of the states through the population of the ground state,

$$\rho_{0,0}^{ee} = \rho_{1,1}^{ee} = \frac{4q^2}{4q^2 + \gamma^2}\rho_{0,0}^{gg}, \quad (23)$$

$$\rho_{1,1}^{gg} = \frac{\gamma^2 + 4p^2}{\gamma^2 + 4q^2}\frac{q^2}{p^2}\rho_{0,0}^{gg}, \quad (24)$$

while $\rho_{0,0}^{gg}$ can be found from the normalization condition.

Let us analyze some limiting cases. We start from the case of a low dissipation, $\gamma \ll p, q$. In this case, the populations of four states are all the same, which is to be expected. In the opposite limit, $\gamma \gg p, q$, we have

$$\rho_{0,0}^{ee} = \rho_{1,1}^{ee} \simeq \frac{4q^2}{\gamma^2}\rho_{0,0}^{gg} \ll \rho_{0,0}^{gg}, \quad (25)$$

$$\rho_{1,1}^{gg} \simeq \frac{q^2}{p^2}\rho_{0,0}^{gg}. \quad (26)$$

We see that in this case the population of the qubit excited state becomes very small, while by tuning the ratio of Fourier components q/p one can redistribute the occupation probability between a state with zero photons and a state with one photon. The higher this ratio, the larger the occupation of the state with one photon. This is a natural result in view of the fact that q is responsible for the excitation from the ground state. What is not so obvious is that $\rho_{1,1}^{gg}$ is dissipation independent, despite the fact that dissipation is needed for this state to be occupied. It is also of interest that the qubit excited state does play a crucial role in this process; nevertheless, it turns out to be essentially empty when a stationary regime is achieved. In order to achieve a ratio q/p exceeding 1, one has to use high-amplitude modulations of $g(t)$, thus changing its sign.

We also consider intermediate cases. The first one is $q \gg \gamma \gg p$. In this case, we obtain

$$\rho_{0,0}^{ee} = \rho_{1,1}^{ee} \simeq \rho_{0,0}^{gg}, \quad (27)$$

$$\rho_{1,1}^{gg} \simeq \frac{\gamma^2}{4p^2} \rho_{0,0}^{gg} \gg \rho_{0,0}^{gg}. \quad (28)$$

The first relation is expected, since we are dealing with the strong excitation limit. However, the second one is not as trivial. It can be understood by the fact that the occupation probability is accumulated in state $|1, g\rangle$ due to the smallness of p , which is responsible for the link with $|0, e\rangle$.

The second intermediate case is $p \gg \gamma \gg q$. It gives

$$\rho_{0,0}^{ee} = \rho_{1,1}^{ee} \simeq \rho_{1,1}^{gg} \simeq \frac{4q^2}{\gamma^2} \rho \ll \rho_{0,0}^{gg}. \quad (29)$$

This situation is rather trivial. It corresponds with weak excitation, so that the occupation probability is accumulated in state $|0, g\rangle$.

The toy model presented in this section is useful since it indicates the general trend of the behavior of our system. Nevertheless, an analysis involving a larger basis of bare states is certainly needed.

Note that by using the interplay between different Fourier components of the external electromagnetic signal, one can also achieve the synchronization of a qubit ensemble [34] despite the unavoidable disorder in excitation energies of Josephson qubits [35].

IV. FULL NUMERICAL ANALYSIS

In this section, we present the results of our numerical simulations of the full set of Eqs. (8) taking into account 80 photon states. We verified the accuracy of this approximation by increasing the number of states taken into account and comparing the results.

We first consider the same modulation, $g(t) = g\theta(\cos 2\omega t)$, as in our previous paper [31], for which $p = 0.5 < q = 1/\pi$. In Fig. 2 we plot the time dependencies of the qubit excited-state population w_e [Fig. 2(a)] and the mean photon number n_{ph} [Fig. 2(b)] after the external driving is turned on at $g_{\max} \equiv \max g(t) = 0.05\omega$, while the initial state had 0 excitations, $|0, g\rangle$. The time is measured as $T_R = \pi/g_{\max}$. Solid lines correspond to the case $\gamma = 0.01\omega$, while dashed lines correspond to $\gamma = 0$. These dependencies are actually superpositions of fast and slow oscillations with frequencies of the order of ω and g_{\max} , respectively. Fast oscillations are not shown in Fig. 2 because of their low amplitude in the limit $g_{\max}/\omega \ll 1$.

It is shown in Fig. 2 that both the qubit excited-state population and the mean photon number tend to experience Rabi-like oscillations, in agreement with the results of [31], but they decay if the nonzero γ is taken into account. Despite the external driving the qubit finally becomes saturated in its ground state. This implies that the dynamical Lamb effect becomes suppressed at long times. However, the mean photon number n_{ph} tends to some nonzero constant value (under the approximation neglecting losses in a photon mode). The characteristic time of the decay of Rabi-like oscillations is

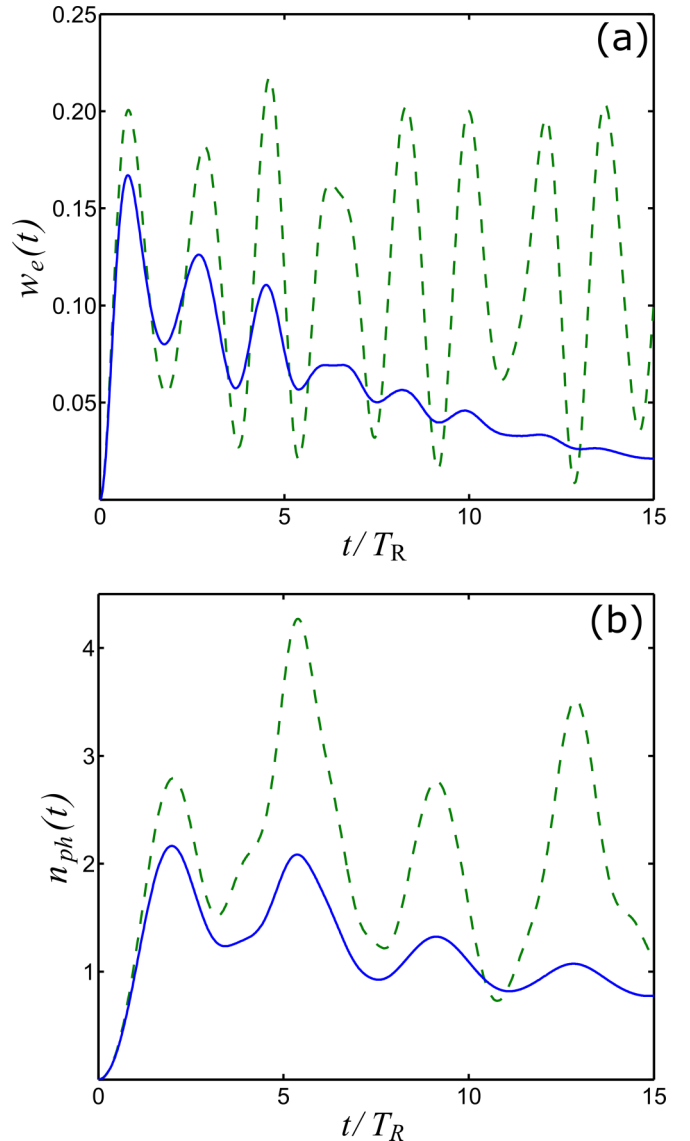


FIG. 2. (a) The qubit excited-state population and (b) the mean photon number as a function of the time after the external parametric driving with $p = 0.5$, $q = 1/\pi$ is turned on at $g_{\max} = 0.05\omega$. Solid blue lines correspond to $\gamma = 0.01\omega$; dashed green lines, to $\gamma = 0$.

given approximately by $1/\gamma$. The nonzero $n_{ph}(t \rightarrow \infty)$ can be treated as a residue of the dynamical Lamb effect, since the photons in the initially empty cavity in the system we study can appear only due to qubit excitation with simultaneous photon creation (term V_2) and subsequent creation of an additional photon and qubit transition to the ground state (term V_1).

The statistics of photon states after their stabilization turns out to be rather peculiar and it is definitely dictated by a parametric excitation of photons. In Fig. 3 we plot the histogram of the dependence of the mean number of photons in the n -photon state on n . We see that only states with even values of n are populated after stabilization. Figure 4 shows how photon states become stabilized after the parametric driving is turned on. The set of parameters for these two figures is the same as that for Fig. 2.

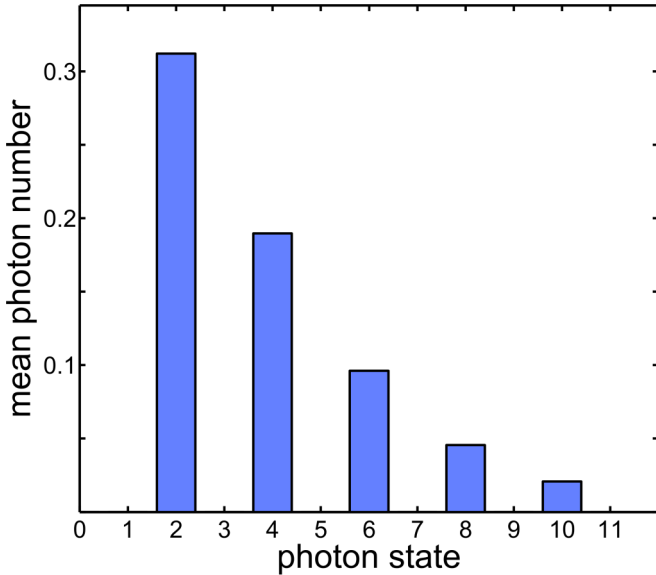


FIG. 3. Histogram of the mean number of photons in n -photon states after stabilization at $\gamma = 0.01\omega$, $g_{\max} = 0.05\omega$. Parameters of the modulation of $g(t)$ are $p = 0.5$, $q = 1/\pi$.

Figures 2 and 3 evidence that only low-energy photon states and the ground-state energy of a qubit are populated after stabilization, i.e., states $|n, g\rangle$ with $n \sim 1$. This is due to the competition between two processes, as shown by the simple toy model presented in the preceding section. The fact that we do have stabilization in our system with the qubit being in its ground state means that the process involving decay is stronger. Nevertheless, in order to achieve this stabilization, as shown in Figs. 2 and 4, a certain intermediate dynamical regime is needed under which the qubit can be in its excited state.

A certain analogy can be seen between this final regime and the phenomenon of parametric down conversion. In both cases, an external pump of the system by a periodic signal results in the spontaneous generation of pairs of photons with lower frequencies. As is known, microscopic mechanisms underlying such nonlinear effects can be different (see, e.g., Ref. [36]). In this paper, we are mainly interested in such a microscopic description of a particular system suitable for realization of the dynamical Lamb effect. Indeed, the main focus of our work is the qubit degrees of freedom, while in the theory of parametric down conversion the main emphasis is on photon generation, whereas the atomic degrees of freedom are normally considered as a source of nonlinearities. Apart from the interest from the viewpoint of fundamental physics, our approach is also motivated by the perspective of using such systems in quantum technologies, in which qubit degrees of freedom as well as correlations between them and photon modes are of crucial importance.

The results obtained by numerical simulations are in qualitative agreement with the results of our toy model in the strong- γ limit at $p > q$. Namely, we see that the qubit excited state tends to become empty, while photon states with a lower energy have larger populations. Of course, the toy model is unable to correctly describe other important features because of the very strong truncation of the basis encoded

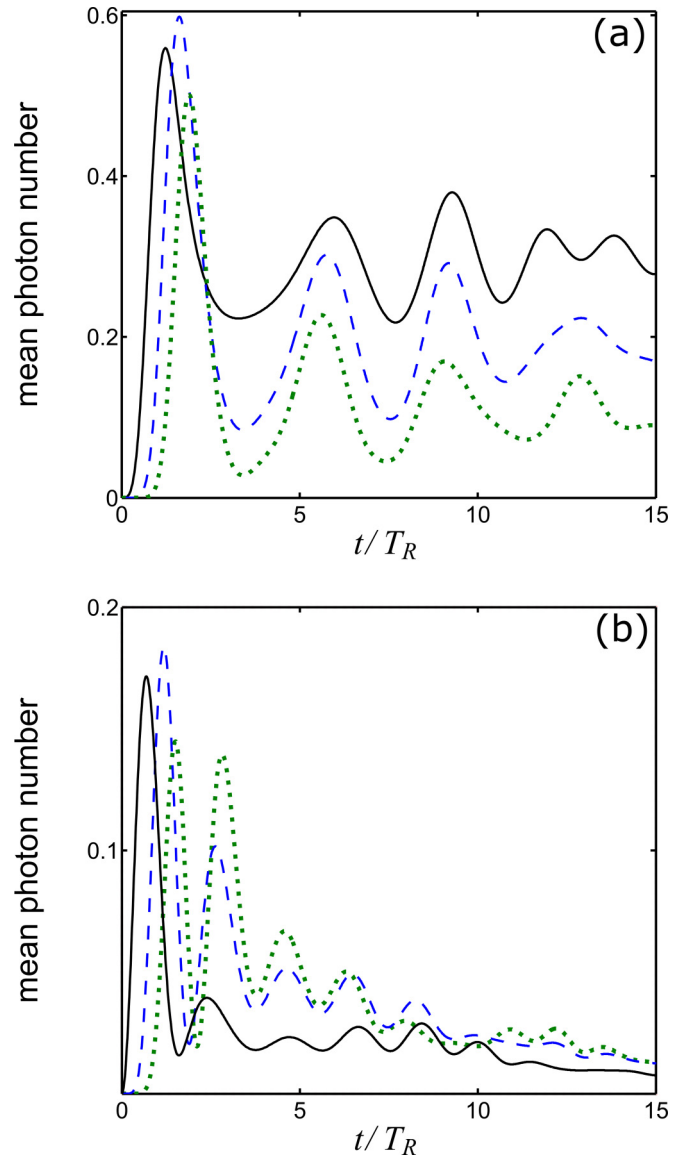


FIG. 4. Dynamics of mean photon numbers in n -photon states with (a) even and (b) odd values of n at $\gamma = 0.01\omega$, $g_{\max} = 0.05\omega$. Parameters of the modulation of $g(t)$ are $p = 0.5$, $q = 1/\pi$. Solid black, dashed blue, and dotted green lines correspond to two-, four-, and six-photon states, respectively, in (a) and to one-, three-, and five-photon states in (b).

in it. For instance, within our toy model, both even and odd photon states are populated in the final state. In order to see how the depletion of odd states occurs at a large enough basis, we extend this basis step by step by taking into account more and more levels and solving the problem numerically. We then follow the evolution of level populations in the final state.

By considering six levels, we see that the population of level $|1, e\rangle$ decreases. The reason is that this occupation probability is redistributed from this level to the “new” state $|2, g\rangle$ through V_1 , while the only channel to increase it is an excitation via V_2 from $|1, g\rangle$ to $|2, e\rangle$, with subsequent decay of the qubit excited state. Since we are in a regime where V_1 overcomes V_2 , the first process dominates and leads to a partial depletion of $|1, e\rangle$. We then see that, due to this mechanism, the larger the basis

we take into account, the stronger the effect of depletion of the qubit excited states. An infinite basis leads to essentially full depletion of these levels. However, in this case, only states with even photon numbers and the qubit in the ground state can be populated, since there is a certain asymmetry between the two subsets of levels with even and odd numbers of photons. Indeed, the “ladder” of states in Fig. 1 starts with 0 (even) number of photons. The state $|0, e\rangle$ can be empty only if $|1, g\rangle$ is empty. Then we can repeat the same argument for $|2, e\rangle$ and $|3, g\rangle$, etc., to see that only populations of states with even photon numbers survive after stabilization.

Note that only even states are also populated under the action of the dynamical Casimir effect. Thus, if generation of Casimir photons is not completely ruled out during an experiment, due to some drawback of the experimental setup, it is difficult to distinguish between the dynamical Lamb effect and the dynamical Casimir effect via photons, provided photon states are studied in experiments at $t \gtrsim 1/\gamma$. Hence, one has to perform measurements within the time interval $\lesssim 1/\gamma$ when both even- and odd-number photon states are populated (as well as the qubit excited state), in contrast to the photon statistics due to the dynamical Casimir effect.

Nevertheless, there is a method to make the dynamical Lamb effect much more pronounced at $t \gtrsim 1/\gamma$. We can see that our toy model predicts some change in the behavior of this type of external drive, for which q exceeds p , which implies the use of sign-alternating time dependences of the coupling constant. We now examine this threshold in numerical simulations. In Fig. 5 we plot the mean photon number in the n -photon state as a function of n at three different moments in time after switching-on of the parametric driving at $p = 0.3$, $q = 1$. We see no stabilization at this ratio of p/q . Namely, the maximum of this dependence increases

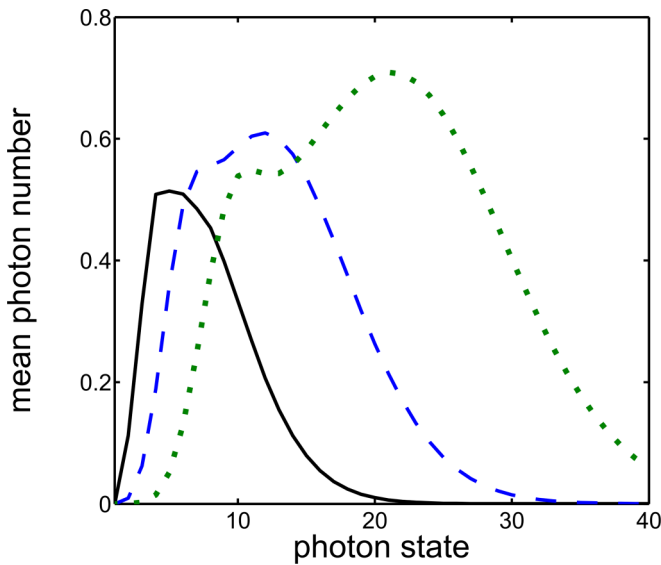


FIG. 5. Dependence of the mean photon number in the n -photon state as a function of n at three moments in time after switching-on of the parametric driving at $\gamma = 0.01\omega$, $g_{\max} = 0.05\omega$. Parameters of modulation of $g(t)$ are $p = 0.3$, $q = 1$. Solid black, dashed blue, and dotted green lines correspond to times T_R , $5T_R$, and $10T_R$, respectively.

with time, so that the total mean photon number also increases. This feature can again be traced from our toy model, which predicts, in the strong- γ limit, certain change in the behavior. The difference is that the toy model includes only four states, so that there is a boundary above which the maximum cannot move. Within the toy model, we see a tendency to maximize the probability of finding a system in the one-photon state, while in reality this maximum starts to move farther. Again, this change in the behavior at $p = q$ can be tested in experiments.

Let us mention that, in the case of a composite system, the possibility of making quantum effects quite robust by using periodic pumping of the coupling constant between its constituent parts was demonstrated in Ref. [37] for two coupled harmonic oscillators at finite and high temperatures. In contrast, we consider a coupled system consisting of two parts which obey Bose and Pauli statistics, respectively, and at low temperatures. Nevertheless, our results together with the results in Ref. [37] indicate that we deal here with a certain class of related phenomena.

Figure 6 shows the time evolution of the qubit excited-state population [Fig. 6(a)] and mean photon number [Fig. 6(b)] after switching-on of the parametric driving characterized by parameters $p = 0.3$, $q = 1$ and at $g_{\max} = 0.05\omega$. Solid lines correspond to a dissipative system with $\gamma = 0.01\omega$; dashed curves, for $\gamma = 0$. We see that the finite value of γ leads to the decay of Rabi-like oscillations for the qubit excited-state population, which tends to be stabilized at the value $1/2$ and does not vanish. Thus, the dynamical Lamb effect is much more robust with respect to dissipation in this case. The most striking feature is that, after some initial oscillations, the mean photon number starts to increase linearly, which shows that there is no stabilization with this type of parametric driving. It is remarkable that this counterintuitive growth is only possible if energy dissipation due to decay of the qubit excited state is present in the system. Indeed, this growth is absent if $\gamma = 0$, as shown in Fig. 6. This happens because another channel of photon generation is open, provided that γ is finite (see Fig. 1). Such a channel does not exist within our toy model because of the basis truncation. It consists in excitation of the initial configuration via V_2 , subsequent decay of the qubit excited state, and, again, excitation of the qubit from the ground to the excited state, with simultaneous photon creation. Hence, both even- and odd-number photon states become populated. Thus, because of the strong increase in the mean photon number, dissipation-assisted parametric amplification of the vacuum occurs.

Let us discuss in more detail the crossover between the two types of behavior which occurs at $p = q$, as deduced from numerics. We continue the set of Eqs. (9)–(14) by taking into account all photon states. We also know that for $\xi = q/p < 1$ at long times, $t \gg 1/\gamma$, only $\rho_{2n, 2n}^{gg}$ is nonzero, while all remaining relevant components vanish. We then equate these quantities to 0 in the new set of equations, as well as the time derivatives $\partial\rho/\partial t$. This leads to the following recurrent relations:

$$\rho_{m+1, n}^{gg} = -\xi \sqrt{\frac{m}{m+1}} \rho_{m-1, n}^{gg}, \quad (30)$$

$$\rho_{m, n+1}^{gg} = -\xi \sqrt{\frac{n}{n+1}} \rho_{m, n-1}^{gg}. \quad (31)$$

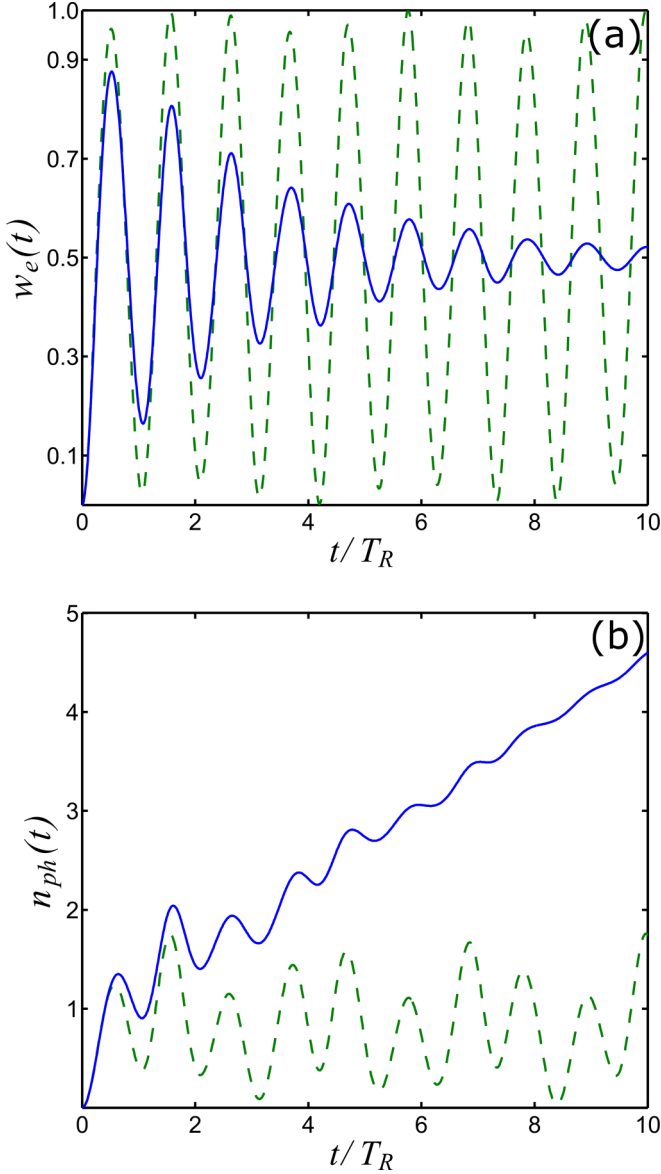


FIG. 6. Dependence of (a) the qubit excited-state population and (b) the mean photon number on the time after switching-on of the parametric driving at $g_{\max} = 0.05\omega$, $p = 0.3$, $q = 1$ at nonzero dissipation $\gamma = 0.01\omega$ (solid blue lines) and at $\gamma = 0$ (dotted green line).

These equations readily yield the identity:

$$\rho_{n+2,n+2}^{gg} = \xi^2 \frac{n+1}{n+2} \rho_{n,n}^{gg}. \quad (32)$$

Starting from $\rho_{0,0}^{gg}$, we obtain

$$\rho_{2j,2j}^{gg} = \xi^{2j} \frac{(2j-1)!!}{(2j)!!} \rho_{0,0}^{gg}, \quad (33)$$

$j = 1, 2, \dots, \infty$. This recurrent relation is in full agreement with our results of numerical simulations for density matrix diagonal components.

In order to determine $\rho_{0,0}^{gg}$, we use the normalization condition $\text{Sp} \rho \equiv 1$, which can be rewritten as

$$\left(1 + \sum_{j=1}^{\infty} \xi^{2j} \frac{(2j-1)!!}{(2j)!!} \right) \rho_{0,0}^{gg} \equiv 1. \quad (34)$$

This series converges provided that $\xi < 1$ or, equivalently, $q < p$; otherwise, normalization is impossible. In the case $\xi < 1$, the result of the summation is

$$\left(1 + \frac{\xi^2}{\sqrt{1-\xi^2}(1+\sqrt{1-\xi^2})} \right) \rho_{0,0}^{gg} \equiv 1, \quad (35)$$

as can be directly checked by performing a Taylor expansion. Thus, the stationary solution indeed exists if the condition $\xi < 1$ is satisfied, while there is no stationary solution at $q \geq p$.

V. EFFECT OF CAVITY RELAXATION

In this section, we take into account cavity dissipation, which is typically much smaller than dissipation of the qubit degrees of freedom in available superconducting qubit-cavity systems. Nevertheless, its effect can be important in view of the fact that different types of dissipation may open various channels in the dynamics of the system, as we have seen in the preceding sections. Thus, we take into account nonzero κ in the Lindblad equation, as given by Eqs. (6) and (7).

We start with consideration of the modulation with $q < p$, for which the qubit excited-state population vanishes at $\kappa = 0$ and at $t \rightarrow \infty$. Figure 7 shows this quantity as a function of time at $p = 0.5$, $q = 1/\pi$, $g_{\max} = 0.05\omega$, $\gamma = 0.01\omega$ and at three values of κ/γ : 0.01 (solid black line), 0.1 (dashed blue line), and 1 (dotted green line). Remarkably, finite cavity dissipation leads to a nonzero qubit excited-state population at long times. This happens because cavity relaxation tends to decrease the mean photon number without changing the

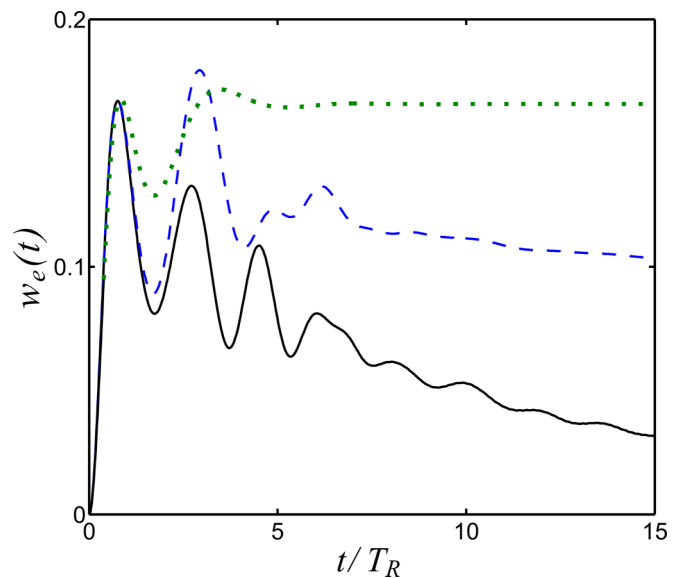


FIG. 7. Qubit excited-state population at $p = 0.5$, $q = 1/\pi$, $g_{\max} = 0.05\omega$, $\gamma = 0.01\omega$ and at three values of κ/γ : 0.01 (solid black line), 0.1 (dashed blue line), and 1 (dotted green line).

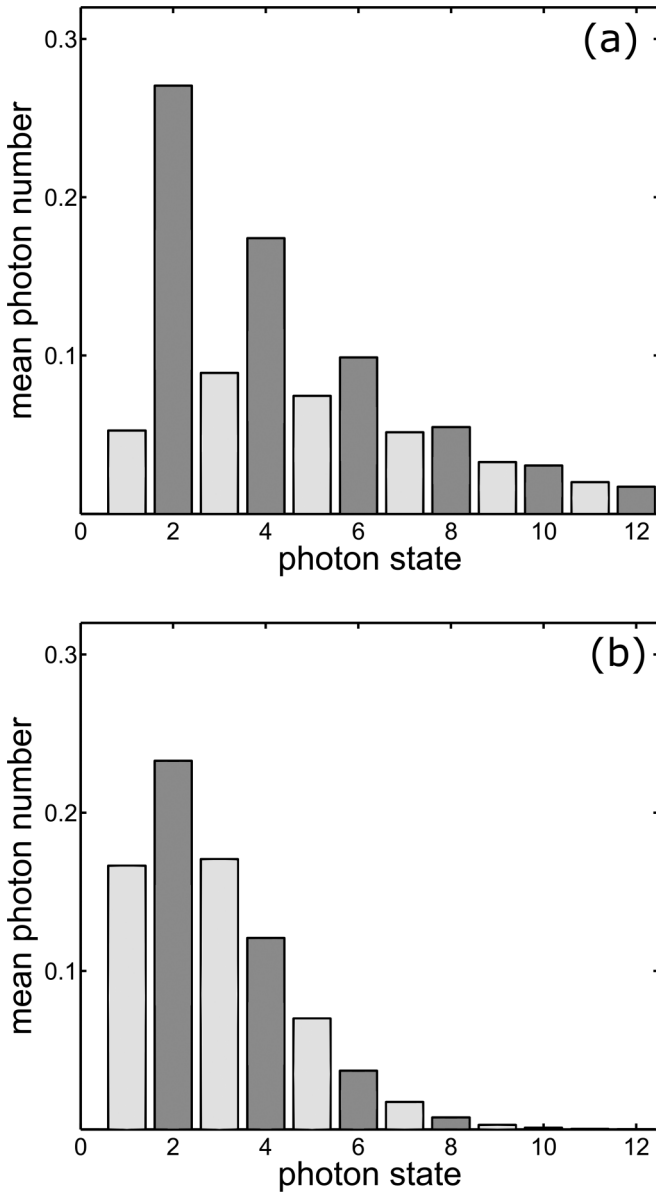


FIG. 8. Histograms of the mean number of photons in n -photon states after stabilization at $\gamma = 0.01\omega$, $g_{\max} = 0.05\omega$ and at two values of κ/γ : (a) 0.1 and (b) 1. Parameters of the modulation of $g(t)$ are $p = 0.5$, $q = 1/\pi$. Dark-gray bars correspond to odd n ; light-gray bars, to even n .

state of the qubit. Therefore, if the qubit is in the excited state, instead of its relaxation to the ground state controlled by γ , the state of the whole system can be changed by decreasing the photon number and keeping the qubit excited. In other words, there is a certain competition between γ and κ in this case. Hence, higher cavity dissipation can also help to increase the qubit excited-state population at $t \rightarrow \infty$, thus supporting the dynamical Lamb effect.

Figure 8 shows histograms of the mean number of photons in n -photon states after stabilization at $\gamma = 0.01\omega$, $g_{\max} = 0.05\omega$, $p = 0.5$, $q = 1/\pi$ and at two values of κ/γ : 0.1 [Fig. 8(a)] and 1 [Fig. 8(b)]. We see that states with odd values of n start to be populated because of the processes which change the photon number without changing the qubit

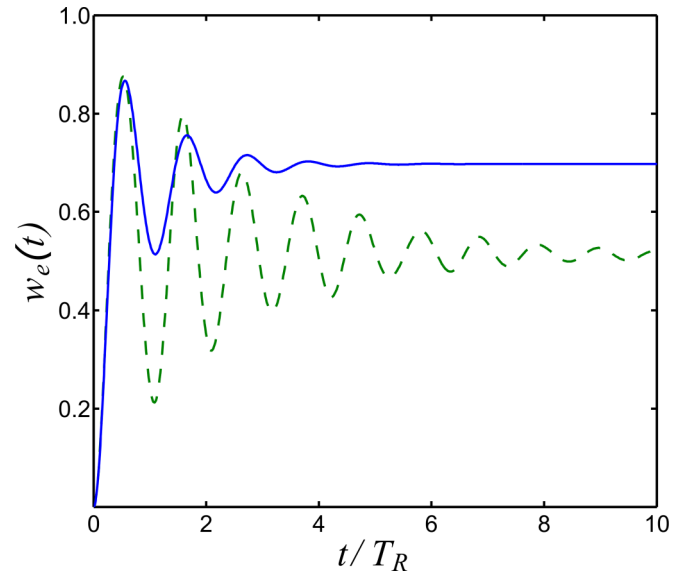


FIG. 9. Qubit excited-state population at $p = 0.3$, $q = 1$, $g_{\max} = 0.05\omega$, $\gamma = 0.01\omega$ and at two values of κ/γ : 1 (solid blue line) and 0.1 (dashed green line).

state. However, the populations of these states remain small at $\kappa/\gamma \ll 1$.

We now consider modulations with $q > p$. Figure 9 shows $w_e(t)$ at two values of κ . We again see that $w_e(t \rightarrow \infty)$ increases as κ increases, but this growth is rather weak at $\kappa/\gamma \ll 1$. This is also due to processes which change the photon number without affecting the qubit degrees of freedom. We again arrive at the same conclusion as in the case where $q < p$: that cavity dissipation increases the dynamical Lamb effect within our scheme at $t \rightarrow \infty$. Actually, these two cases, $q > p$ and $q < p$, become not so distinct when a nonzero κ is taken into account, as can be expected. Indeed, Fig. 10 shows the mean photon number as a function of time for three values of κ . The nearly linear growth of this quantity at $t \rightarrow \infty$ found for $\kappa = 0$ is replaced by its saturation. Its final value drops as κ increases. However, it still can be much larger than the same quantity in the absence of dissipation, which implies that an additional channel of photon generation from vacuum with the assistance of qubit relaxation, as discussed in the preceding section, still exists in this $\kappa \neq 0$ case.

The major result in this section is that nonzero cavity dissipation increases the qubit excited-state population at $t \rightarrow \infty$. This feature can be used as an alternative tool to increase the effect without switching to sign-alternating modulations, which can be difficult to implement in experiments.

Let us mention that some aspects of the temporary evolution of systems with dynamically tunable light-matter interactions have been studied in the literature (see, e.g., Refs. [25–27,38–41]). This interaction was assumed to vary either along or simultaneously with other parameters, such as the cavity frequency. In most of these studies, however, only a regime of weak modulation was considered. In general, it was also implicitly suggested that the dissipation rates of both qubit and photon states are of the same order. Due to these assumptions, a rich dynamical picture, predicted in the present paper, has not been revealed up to now, to the best of

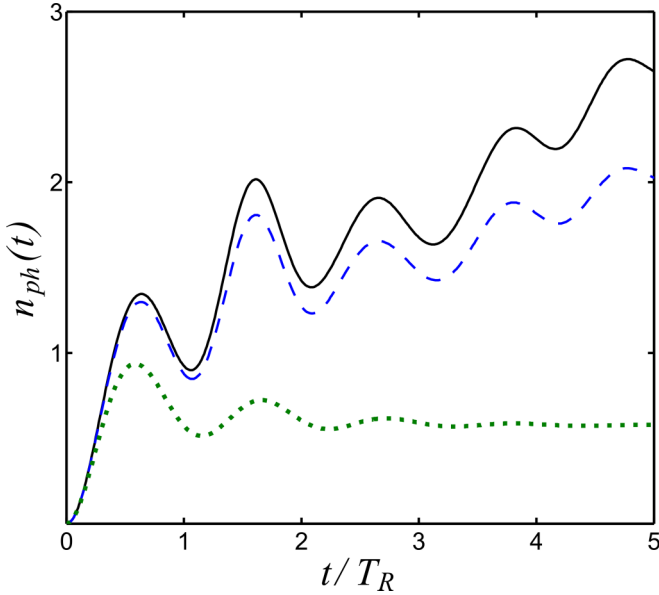


FIG. 10. Mean photon number at $p = 0.3$, $q = 1$, $g_{\max} = 0.05\omega$, $\gamma = 0.01\omega$ and at three values of κ/γ : 0.01 (solid black line), 0.1 (dashed blue line), and 1 (dotted green line).

our knowledge. Moreover, as usual in the case of nonlinear optical effects, these studies focused mainly on the analysis of properties of photons generated upon the modulation of system parameters. For instance, in Ref. [27] the interaction between Casimir photons and matter was shown to be responsible for the nonlinear-in-photon-number term in the purely photonic effective Hamiltonian in certain limits. The latter was obtained by exclusion of the atomic degrees of freedom from the full “microscopic” system Hamiltonian. Within this approach, the term *nonlinear dynamical Casimir effect* was introduced in Ref. [27]. In contrast, the present paper as well as preceding articles [22,23,31] concentrate mainly on what goes on with the qubit (atom) degrees of freedom. From this perspective, the nonlinear dynamical Casimir effect in a nonstationary cavity is intrinsically related to the atom excitation due to absorption of Casimir photons as well as to the dynamical Lamb effect.

VI. NUMERICAL SOLUTION FOR STEADY-STATE LIMIT

In this section, we provide an alternative approach to the problem, which enables us to directly attain the steady-state limit achieved after stabilization of the system and to cross-check our results. The solution for the density matrix elements in the steady-state limit, i.e., on time scales significantly exceeding the relaxation times, can be found numerically without direct integration over the entire evolution period. This calculation can be performed by means of integration of the Lindblad equation over a single period of the time-dependent Hamiltonian $H(t)$, i.e., within the interval $0 < t < \pi/\omega$. In this solution we do not perform integrating-out of fast-oscillating terms and do not use transition to rotating frames.

The Lindblad equation can be rewritten through the supermatrix $A(t)$ acting on vector $\vec{\rho}(t)$ combined from elements of the density matrix $\rho(t)$,

$$d\vec{\rho}(t)/dt = A(t)\vec{\rho}(t). \quad (36)$$

In the steady-state limit we assume that this solution is periodic $\vec{\rho}(t + \pi/\omega) = \vec{\rho}(t)$, with the period $T = \pi/\omega$ of Hamiltonian $H(t)$ and $A(t)$. We find numerically the matrix of evolution U , which relates $\vec{\rho}(T)$ and $\vec{\rho}(0)$:

$$\vec{\rho}(T) = U\vec{\rho}(0). \quad (37)$$

The eigenvector of $\vec{\rho}_0 = U\vec{\rho}_0$ gives the steady-state solution $\vec{\rho}_0 = \vec{\rho}(NT)$ realized at infinite limit of N . Integration of the Lindblad equation over $0 < t < \pi/\omega$ with the initial condition $\vec{\rho}_0$ provides the periodic steady solution $\rho_{st}(t)$. Averaging of the diagonal elements of $\rho_{st}(t)$ over the time provides the level populations in the qubit and photon channels. This solution gives mean photon numbers which are identical to the above results for the time-dependent numerical solution.

VII. SUMMARY AND CONCLUSIONS

The coupled system of a superconducting qubit and a microwave resonator can be used for experimental observation of the dynamical Lamb effect [31], which can be treated as the parametric excitation of an atom due to nonadiabatical modulation of its Lamb shift [23]. This can be achieved by dynamically tuning the vacuum Rabi frequency (strength of the coupling between qubit and resonator) without changing any other parameters, such as the resonator frequency. Under these conditions, no generation of Casimir photons occurs, which is a crucial condition for isolation of the dynamical Lamb effect from other nonstationary QED phenomena also leading to the parametric excitation of a qubit. This modulation of the vacuum Rabi frequency in superconducting circuits is possible thanks to several approaches proposed recently [28–30]. Note that, in contrast to natural systems, it is also possible to achieve a regime of strong or even ultrastrong light-matter coupling in artificial superconducting systems.

In the present paper we have studied the influence of energy dissipation on qubit excitation due to the dynamical Lamb effect. The influence of dissipation in a qubit is of particular importance since it leads to qubit de-excitation and it also far exceeds cavity relaxation in typical superconducting qubit-cavity systems.

Our major conclusion is that the qubit excited-state population in the presence of dissipation depends crucially on the character of the vacuum Rabi frequency modulation. Note that we have assumed that the qubit and resonator in the initial moment are not excited. We also took into account that decay of photon states in superconducting circuits is typically much weaker than relaxation in a qubit, which allows for the separation of the characteristic time scales for the two types of dissipation.

We found that some types of periodic modulation of the vacuum Rabi frequency lead to a decay with time of the qubit excited-state population, while the mean number of generated photons tends to be stabilized around some finite number. However, other types of parametric driving of the same quantity lead to completely different behavior. In this case, the qubit excited-state population becomes stabilized near the large value of 1/2, while the number of photons in the system increases nearly linearly with time until it also becomes stabilized by photon-field relaxation. Hence, in this case, the dynamical Lamb effect is much more robust with

respect to dissipation in a qubit. The latter phenomenon can be treated as dissipation-assisted parametric amplification of a vacuum, since another channel of photon generation from the vacuum opens due to the relaxation of the qubit.

We would like to stress that this striking increase in the photon number is possible only when finite dissipation in a qubit is taken into account, since this dissipation adds another channel of photon generation from vacuum via the qubit degrees of freedom. These results show that there are two competing processes in our system. The first one is due to counter-rotating processes, which excite the qubit, with simultaneous photon creation. The second one is decay of the qubit excited state accompanied by oscillations due to excitation-number-conserving processes. Which one prevails depends on the character of the modulation. We also demonstrate that this competition can be described by the balance of two parameters which are nothing but two first Fourier components of the vacuum Rabi frequency as a function of the time. The second regime is possible only for strong driving, such that the coupling constant changes its sign during modulation. Modulation of this sort seems possible with present or near-future technologies. Thus, we hope that the change in behavior that we predict here can be observed in experiments.

We have also analyzed in more detail the effect of cavity relaxation. We find that the difference between the two regimes is smeared out, since in both cases stabilization is finally achieved, but only at long enough times. Moreover, nonzero cavity relaxation always leads to an enhancement of the qubit excited-state population at long times. Hence, by increasing

this quantity, one can also increase the dynamical Lamb effect. This increase is stronger for those types of modulation which lead to the decay of this probability in the dissipation-free case. Thus, an increase in cavity relaxation provides an alternative method for enhancing the effect. This method is important because it does not require the use of sign-alternating modulations, which can be technically difficult to implement.

The investigation of responses of quantum systems to nonadiabatic modulation of their parameters is of interest not only from the viewpoint of realization of various fundamental QED effects, but also for the purposes of quantum computation. Indeed, high-speed gates can induce various nonstationary QED effects related to vacuum amplification and parametric generation of excitations from vacuum. Therefore, both the understanding and the control of such effects are of great importance.

ACKNOWLEDGMENTS

The authors acknowledge useful comments by A. V. Ustinov, O. V. Astafiev, K. V. Shulga, E. S. Andrianov, S. V. Remizov, and L. V. Bork. W.V.P. acknowledges financial support by RFBR (Project No. 15-02-02128) and by Ministry of Education and Science of the Russian Federation (Grant No. 14.Y26.31.0007). Work of D.S.S. was supported by the Fellowship of the President of Russian Federation for young scientists (fellowship no. SP-2044.2016.5). Results of Section VI were derived by D.S.S. with financial support from the Russian Science Foundation (Contract No. 16-12-00095). Yu. E. L. was supported by the Program of Basic Research of HSE.

-
- [1] P. D. Nation, J. R. Johansson, M. P. Blencowe, and F. Nori, Colloquium: Stimulating uncertainty: Amplifying the quantum vacuum with superconducting circuits, *Rev. Mod. Phys.* **84**, 1 (2012).
- [2] M. H. Devoret, S. Girvin, and R. J. Schoelkopf, How strong can the coupling between a Josephson junction atom and a transmission line resonator be? *Ann. Phys. (Leipzig)* **16**, 767 (2007).
- [3] O. Astafiev, A. M. Zagoskin, A. A. Abdumalikov, Jr., Yu. A. Pashkin, T. Yamamoto, K. Inomata, Y. Nakamura, and J. S. Tsai, Resonance fluorescence of a single artificial atom, *Science* **327**, 840 (2010).
- [4] G. Oelsner, P. Macha, O. V. Astafiev, E. Il'ichev, M. Grajcar, U. Hübner, B. I. Ivanov, P. Neilinger, and H.-G. Meyer, Dressed-State Amplification by a Single Superconducting Qubit, *Phys. Rev. Lett.* **110**, 053602 (2013).
- [5] R. Barends, L. Lamata, J. Kelly, L. Garcia-Alvarez, A. G. Fowler, A. Megrant, E. Jeffrey, T. C. White, D. Sank, J. Y. Mutus, B. Campbell, Y. Chen, Z. Chen, B. Chiaro, A. Dunsworth, I.-C. Hoi, C. Neill, P. J. J. O'Malley, C. Quintana, P. Roushan, A. Vainsencher, J. Wenner, E. Solano, and J. M. Martinis, Digital quantum simulation of fermionic models with a superconducting circuit, *Nat. Commun.* **6**, 7654 (2015).
- [6] A. D. Crocoles, E. Magesan, Srikanth J. Srinivasan, A. W. Cross, M. Steffen, J. M. Gambetta, and J. M. Chow, Demonstration of a quantum error detection code using a square lattice of four superconducting qubits, *Nat. Commun.* **6**, 6979 (2015).
- [7] J. Braumüller, M. Sandberg, M. R. Vissers, A. Schneider, S. Schlör, L. Grünhaupt, H. Rotzinger, M. Marthaler, A. Lukashenko, A. Dieter, A. V. Ustinov, M. Weides, and D. P. Pappas, Concentric transmon qubit featuring fast tunability and an anisotropic magnetic dipole moment, *Appl. Phys. Lett.* **108**, 032601 (2016).
- [8] Yu. Makhlin, G. Schön, and A. Shnirman, Quantum-state engineering with Josephson-junction devices, *Rev. Mod. Phys.* **73**, 357 (2001).
- [9] P. Lähteenmäki, G. S. Paraoanu, J. Hassel, and P. J. Hakonen, Dynamical Casimir effect in a Josephson metamaterial, *Proc. Natl. Acad. Sci. USA* **110**, 4234 (2013).
- [10] C. M. Wilson, G. Johansson, A. Pourkabirian, J. R. Johansson, T. Duty, F. Nori, and P. Delsing, Observation of the dynamical Casimir effect in a superconducting circuit, *Nature* **479**, 376 (2011).
- [11] G. T. Moore, Quantum theory of the electromagnetic field in a variable-length one-dimensional cavity, *J. Math. Phys.* **11**, 2679 (1970).
- [12] A. Fragner, M. Goppl, J. M. Fink, M. Baur, R. Bianchetti, P. J. Leek, A. Blais, and A. Wallraff, Resolving vacuum fluctuations in an electrical circuit by measuring the Lamb shift, *Science* **322**, 1357 (2008).

- [13] E. Yablonovitch, Accelerating Reference Frame for Electromagnetic Waves in a Rapidly Growing Plasma: Unruh-Davies-Fulling-De Witt Radiation and the Nonadiabatic Casimir Effect, *Phys. Rev. Lett.* **62**, 1742 (1989).
- [14] Yu. E. Lozovik, V. G. Tsvetus, and E. A. Vinogradov, Parametric excitation of vacuum by use of femtosecond laser pulses, *Phys. Scripta* **52**, 184 (1995).
- [15] A. V. Dodonov, E. V. Dodonov, and V. V. Dodonov, Photon generation from vacuum in nondegenerate cavities with regular and random periodic displacements of boundaries, *Phys. Lett. A* **317**, 378 (2003).
- [16] C. Braggio, G. Bressi, G. Carugno, C. Del Noce, G. Galeazzi, A. Lombardi, A. Palmieri, G. Ruoso, and D. Zanello, A novel experimental approach for the detection of the dynamical Casimir effect, *Europhys. Lett.* **70**, 754 (2005).
- [17] E. Segev, B. Abdo, O. Shtempluck, E. Buks, and B. Yurke, Prospects of employing superconducting stripline resonators for studying the dynamical Casimir effect experimentally, *Phys. Lett. A* **370**, 202 (2007).
- [18] W. G. Unruh, Notes on black-hole evaporation, *Phys. Rev. D* **14**, 870 (1976).
- [19] S. W. Hawking, Particle creation by black holes, *Commun. Math. Phys.* **43**, 199 (1975).
- [20] D. J. Heinzen and M. S. Feld, Vacuum Radiative Level Shift and Spontaneous-Emission Linewidth of an Atom in an Optical Resonator, *Phys. Rev. Lett.* **59**, 2623 (1987).
- [21] A. A. Belov, Yu. E. Lozovik, and V. L. Pokrovsky, Lamb shift of Rydberg atoms in a resonator, *J. Phys. B* **22**, L101 (1989).
- [22] A. M. Fedotov, N. B. Narozhny, and Yu. E. Lozovik, 'Shaking' of an atom in a nonstationary cavity, *Phys. Lett. A* **274**, 213 (2000).
- [23] N. B. Narozhny, A. M. Fedotov, and Yu. E. Lozovik, Dynamical Lamb effect versus dynamical Casimir effect, *Phys. Rev. A* **64**, 053807 (2001).
- [24] H. Walther, B. T. H. Varcoe, B. G. Englert, and T. Becker, Cavity quantum electrodynamics, *Rep. Prog. Phys.* **69**, 1325 (2006).
- [25] V. V. Dodonov, Current status of the dynamical Casimir effect, *Phys. Scripta* **82**, 038105 (2010).
- [26] D. S. Veloso and A. V. Dodonov, Prospects for observing dynamical and anti-dynamical Casimir effects in circuit QED due to fast modulation of qubit parameters, *J. Phys. B* **48**, 165503 (2015).
- [27] I. M. de Sousa and A. V. Dodonov, Microscopic toy model for the cavity dynamical Casimir effect, *J. Phys. A* **48**, 245302 (2015).
- [28] S. J. Srinivasan, A. J. Hoffman, J. M. Gambetta, and A. A. Houck, Tunable Coupling in Circuit Quantum Electrodynamics Using a Superconducting Charge Qubit with a V-Shaped Energy Level Diagram, *Phys. Rev. Lett.* **106**, 083601 (2011).
- [29] A. J. Hoffman, S. J. Srinivasan, J. M. Gambetta, and A. A. Houck, Coherent control of a superconducting qubit with dynamically tunable qubit-cavity coupling, *Phys. Rev. B* **84**, 184515 (2011).
- [30] S. Zeytinoglu, M. Pechal, S. Berger, A. A. Abdumalikov, Jr., A. Wallraff, and S. Filipp, Microwave-induced amplitude- and phase-tunable qubit-resonator coupling in circuit quantum electrodynamics, *Phys. Rev. A* **91**, 043846 (2015).
- [31] D. S. Shapiro, A. A. Zhukov, W. V. Pogosov, and Yu. E. Lozovik, Dynamical Lamb effect in a tunable superconducting qubit-cavity system, *Phys. Rev. A* **91**, 063814 (2015).
- [32] I. I. Rabi, Space quantization in a gyrating magnetic field, *Phys. Rev.* **51**, 652 (1937).
- [33] E. T. Jaynes and F. W. Cummings, Comparison of quantum and semiclassical radiation theories with application to the beam maser, *Proc. IEEE* **51**, 89 (1963).
- [34] S. V. Remizov, D. S. Shapiro, and A. N. Rubtsov, Synchronization of qubit ensembles under optimized π -pulse driving, *Phys. Rev. A* **92**, 053814 (2015).
- [35] D. S. Shapiro, P. Macha, A. N. Rubtsov, and A. V. Ustinov, Dispersive response of a disordered superconducting quantum metamaterial, *Photonics* **2**, 449 (2015).
- [36] R. W. Boyd, *Nonlinear Optics*, 3rd ed. (Academic Press, New York, 2008).
- [37] F. Galve, L. A. Pachón, and D. Zueco, Bringing Entanglement to the High Temperature Limit, *Phys. Rev. Lett.* **105**, 180501 (2010).
- [38] S. De Liberato, D. Gerace, I. Carusotto, and C. Ciuti, Extracavity quantum vacuum radiation from a single qubit, *Phys. Rev. A* **80**, 053810 (2009).
- [39] L. Garziano, A. Ridolfo, R. Stassi, O. Di Stefano, and S. Savasta, Switching on and off of ultrastrong light-matter interaction: Photon statistics of quantum vacuum radiation, *Phys. Rev. A* **88**, 063829 (2013).
- [40] G. Benenti, S. Succi, and G. Strini, Exotic states in the dynamical Casimir effect, *Eur. Phys. J. D* **68**, 139 (2014).
- [41] W. Kopylov, C. Emary, E. Schöll, and T. Brandes, Time-delayed feedback control of the Dicke-Hepp-Lieb superradiant quantum phase transition, *New J. Phys.* **17**, 013040 (2015).